Estimating waterbird abundance on catfish aquaculture ponds using an unmanned aerial system

Paul C. Burr, Mississippi State University, Department of Wildlife, Fisheries, and Aquaculture, Box 9680, Mississippi State, MS 39762, USA *Pcb124@msstate.edu*

Sathishkumar Samiappan, Geosystems Research Institute, Mississippi State University, Box 9627, Mississippi State, MS 39762, USA

Lee A. Hathcock, Geosystems Research Institute, Mississippi State University, Box 9627, Mississippi State, MS 39762, USA

Robert J. Moorhead, Geosystems Research Institute, Mississippi State University, Box 9627, Mississippi State, MS 39762, USA

Brian S. Dorr, USDA, APHIS, Wildlife Services' National Wildlife Research Center, Mississippi Field Station, 2745 West Line Road, Mississippi State, MS 39762, USA

Abstract: In this study, we examined the use of an unmanned aerial system (UAS) to monitor fish-eating birds on catfish (*Ictalurus* spp.) aquaculture facilities in Mississippi, USA. We tested 2 automated computer algorithms to identify bird species using mosaicked imagery taken from a UAS platform. One algorithm identified birds based on color alone (color segmentation), and the other algorithm used shape recognition (template matching), and the results of each algorithm were compared directly to manual counts of the same imagery. We captured digital imagery of great egrets (*Ardea alba*), great blue herons (*A. herodias*), and double-crested cormorants (*Phalacrocorax auritus*) on aquaculture facilities in Mississippi. When all species were combined, template matching algorithm produced an average accuracy of 0.80 (SD = 0.58), and color segmentation algorithm produced an average accuracy of 0.67 (SD = 0.67), but each was highly dependent on weather, image quality, habitat characteristics, and characteristics of the birds themselves. Egrets were successfully counted using both color segmentation and template matching. Template matching performed best for great blue herons compared to color segmentation, and neither algorithm performed well for cormorants. Although the computer-guided identification in this study was highly variable, UAS show promise as an alternative monitoring tool for birds at aquaculture facilities.

Key words: aquaculture, *Ardea alba, Ardea herodias,* catfish, cormorant, drone, egret, heron, *Ictalurus* spp., *Phalacrocorax auritus*, unmanned aerial system

Manned aircraft have been traditionally used to conduct aerial surveys of wildlife in large areas where ground surveys would be too costly or impractical. Although these aerial surveys are effective, they have limitations in terms of the high costs associated with the purchase or lease of planes and operational costs such as fuel and staff and pilot labor. Also, considerable expertise and training are required of pilots and staff to meet operational needs and reduce the risk of injury or even death in one of the more hazardous endeavors in the wildlife profession (Sasse 2003). Manned aircraft are also known for disturbing wildlife during low altitude surveys (Christie et al. 2016) and often result in biased estimates due to observer subjectivity (Frederick et al. 1996, Green et al. 2008, Bakó et al. 2014). Unmanned aerial systems (UAS) are a rapidly advancing

tool that may be used to address some of the issues associated with these legacy approaches to aerial survey methods (Linchant et al. 2015).

A UAS is an unmanned motorized aerial vehicle platform that is capable of flying autonomously, semi-autonomously, or manually by a ground-based pilot using a radio frequency-based remote control and a ground control station. Different UAS platforms have unique capabilities and limitations associated with the payload or the type of sensor being carried, total flight time, and maximum and minimum altitude (Anderson and Gaston 2013). To record the trajectory of flight, a UAS platform has an integrated navigation system based on global position system (GPS) satellites, inertial navigation system, an altimeter, and a directional compass (Samiappan et al. 2017). Small UAS open new possibilities such as near

real-time, low-cost aerial surveying and high-resolution image capture as an economically and ecologically viable alternative to classical manned aerial methods (Anderson and Gaston 2013, Linchant et al. 2015, Hodgson et al. 2016, Han et al. 2017). From an ecological perspective, UAS have wide-ranging applications including collection of wildlife abundance and distribution information, reproductive estimation, and habitat data metrics, all while being potentially less invasive and cheaper alternatives to classical manned aircraft methods (Anderson and Gaston 2013, Christie et al. 2016). Additionally, UAS offer an alternative to ground-based abundance estimates. Hodgson et al. (2018) found abundance estimates taken from UAS imagery to be more accurate than ground-based counting.

Currently, UAS are limited to use in areas smaller in scale than typical manned aerial survey methods. As technology and regulatory requirements change, their range could be significantly expanded. However, a small UAS platform may still be used as an effective survey method at smaller scales than traditional aerial survey methods or in specific situations where access is limited or when less invasive monitoring methods are preferred (Christie et al. 2016). For example, UAS have been used numerous times to monitor colonial birds, a group of species that are sensitive to disturbance and are often found in areas difficult to access (Sardà-palomera et al. 2017, Rush et al. 2018). Sardà-palomera et al. (2017) were even able to collect data on nest success based on distance to nearest incubating neighbor of black-headed gulls (*Chroicocephalus ridibundus*) using UAS on a remote island. High-resolution imagery collected from UAS platforms also provides the opportunity for computer-guided algorithms to identify target organisms, eliminating the time-consuming task of manual counting. This application is already showing promising results in wildlife monitoring (Abd-Elrahman et al. 2005, Linchant et al. 2015). The benefits of low altitude sensing with high-resolution optical sensors and computer vision algorithms to precisely identify and measure ground targets make UAS a potentially useful wildlife monitoring tool.

We employed a relatively small, inexpensive UAS platform capable of collecting geo-referenced high-resolution imagery to conduct surveys of fish-eating birds on selected catfish (*Ictalurus* spp.) aquaculture facilities in the primary aquaculture producing areas of Mississippi, USA. Considerable research effort has been expended on determining potential economic impacts of fish-eating birds on the catfish aquaculture industry (Glahn and Brugger 1995, Glahn et al. 2000, Glahn and King 2004, Dorr et al. 2012). A key component in determining the extent of depredation and loss has been the distribution of fish-eating birds on farm ponds, the proportion of farm ponds utilized, and the type or condition of ponds utilized. Proportional use and count information are essential in determining the economic impact of fish-eating birds to the catfish aquaculture industry (Dorr et al. 2008, 2012). Historically, these surveys have been conducted from the ground or by air using certified pilots, typically in fixed-wing aircraft. Platforms such as UAS may be a useful alternative to assess damage to agricultural commodities from many sources, including wildlife. Our goal was to evaluate the resolution and extent of coverage necessary to provide for UAS remotely-sensed and pattern recognition-based censuses of fish-eating birds.

The objectives of this research work were to: (1) develop and implement a field data collection protocol for evaluating the ability of small, relatively inexpensive and readily available UAS to detect and identify fish-eating birds at aquaculture facilities; (2) evaluate the suitability and accuracy of visible spectrum imagery ranging from approximately 1–4 cm resolutions for automated pattern recognition of waterbird species; and (3) determine the efficiency of automated pattern recognition methods versus manual counting methods from UAS-based image mosaics.

Study area

Mississippi is the leading producer of catfish in the United States, and currently the catfish aquaculture industry is the state's fifth largest agriculture commodity (Vilsack and Reilly 2014). Most catfish production occurs within an 18,000-km^2 region located in the northwest portion of the state, known as the Mississippi Delta (Vilsack and Reilly 2014, National Agricultural Statistics Service [NASS] 2015).

Catfish are cultured here in large pond systems averaging 3.5 ha in size (U.S. Department of Agriculture [USDA] 2010). The majority of ponds are open to the environment, which readily prompts conflict between producers and wildlife. Damages and economic losses attributed to fish-eating birds on catfish facilities have been a primary and continuous problem in this region (Tucker and Hargreaves 2004). Therefore, to address our objectives, we surveyed selected catfish farms within the Mississippi Delta. Our goal was to collect imagery of the most commonly documented avian predators of catfish in the region on aquaculture ponds. These species include double-crested cormorants (*Phalacrocorax auritus;* hereafter, cormorant), great blue herons *(Ardea herodias*; hereafter, heron), and great egrets (*A. alba*; hereafter, egret; Mott and Brunson 1995, Glahn and King 2004).

Methods

The PrecisionHawk Lancaster (PrecisionHawk, Raleigh, North Carolina, USA) and Robota Triton (Robota, Dallas, Texas, USA) UAS platforms were used to collect visible imagery at different heights above ground level (AGL) from 3 different catfish aquaculture facilities in the Mississippi Delta. These 3 catfish facilities were opportunistically chosen based on accessibility and known bird presence.

Study area 1 was located north of Leland, Mississippi, in Washington County (-90.891425°, 33.447374°), covered an area of approximately 20 ha, and contained 35 ponds with a mean area of 0.29 ha (SD = 0.12). Imagery from flights at 61 m, 122 m, and 183 m AGL were collected using a visible Sony RX100 20MP camera (Sony, San Diego, California, USA) on a Robota Triton UAS. Flight durations for each height AGL were approximately 50, 45, and 30 minutes, respectively. For this study, we defined a survey as a single day of image collection at a given study area. We surveyed study area 1 on September 8, 2014, in which only the 122 m AGL was flown. This was the only instance in which all 3 heights were not flown for a given survey. We later surveyed study area 1 again on October 18, 2014 and collected data at all 3 heights. All data from both of these surveys were included in subsequent analysis. The ground resolution corresponding to the UAS flown at heights 61 m, 122 m, and 183 m were approximately 1.2 cm, 2.5 cm, and 3.5 cm, respectively.

Study area 2 was located south of Indianola, Mississippi in Humphrey County (-90.539764°, 33.327089°), covered an area of approximately 35 ha, and contained 6 ponds with a mean area of 3.91 ha (SD = 1.41). This imagery was collected on March 24, 2015, using the same camera and heights AGL as area 1, and flight durations were approximately 35, 30, and 25 minutes, respectively.

Study area 3 was located west of Greenwood, Mississippi at the border of Leflore and Sunflower Counties (-90.447358°, 33.589214°) and surveyed on March 17, 2016. Study area 3 covered an area of approximately 65 ha and contained 11 ponds with an average area of 4.56 ha (SD = 1.79). Imagery was collected with a visible Sony RX100 camera using the Triton UAS at 122 m and 183 m AGL. We were unable to use the Triton UAS for the 61 m AGL flight due to damage; we therefore used a visible Nikon camera (Nikon Inc. Melville, New York, USA) on the Lancaster UAS to give the same ground sample distance as the Sony RX100.

Although there are minor differences between these UAS platforms and cameras (discussed below), the resulting imagery and resolution produced were comparable and were therefore not treated differently. Flight durations were 74, 26, and 19 minutes, respectively. During each survey, the data for each height AGL were collected on the same day but almost 2 hours apart from each other, so the position and the number of birds at each height AGL varied. Egrets and herons were observed only at study area 1, and cormorants were observed at areas 2 and 3.

The Lancaster and Triton weigh approximately 7 kg and 5 kg with payload, respectively, and have a 2.7-m wingspan and 1.5-m length. Both of these UAS platforms are fixed wing, single electric motor, and a mix of Styrofoam™ and either plastic or printed circuit board construction (Triton and Lancaster, respectively) fully autonomous planes that can be hand-launched and capable of capturing imagery on flights lasting up to 25 minutes for the Lancaster and 45 minutes for the Triton. They both cruise at approximately 50 km per hour. The Lancaster utilizes ArduPilot, an open source UAS system sold by 3D Robotics (DYI

Drones, Berkeley, California, USA) to create and monitor georeferenced flight plans. The optimal flight plan for imagery collection is automatically estimated by using the onboard flight computer depending on the shape of the survey area, wind speed, and wind direction. This optimization happens after the launch and once the aircraft reaches the predetermined height AGL to account for real-time local weather conditions. The Triton uses its own solution, the Goose autopilot, developed in-house at Robota. It allows the explicit flight lines to be set up within their ground control station (GCS) software.

The Lancaster uses an open source GCS (similar to a flight instrument) application called Mission Planner (DYI Drones, Berkeley, California, USA) that provides live information about the flight mission, such as the height AGL, airspeed, and remaining energy in the battery. Mission Planner is based on the ArduPilot open source autopilot project that helps set up, configure, and tune the UAS for optimum performance. Mission Planner is capable of loading and saving the flight plans to the onboard aircraft computer with the point-and-click entry of way-points on Google or Bing maps. The Triton GCS accomplishes the same purpose but is based on internally developed software at Robota and communicates only with the Goose autopilot.

In this study, we sought to use visible spectrum imagery so that it can be compared with direct human manual counting. Individual images obtained from each flight were mosaicked on a per-flight basis using Agisoft Photoscan Pro (Agisoft LLC, St. Petersburg, Russia). The UAS onboard computer stores the latitude, longitude, and height AGL of the aircraft for each image taken along with other telemetry information. This information was uploaded to Photoscan Pro to give initial camera positions and to perform georeferencing. Individual images with 60% side overlap and 60% forward overlap were used for creating the image mosaics, which were typically produced at the high quality setting for alignment using the sparse cloud and a high quality mesh. The orthomosaic was then exported in a tiled format and stitched together into a large image mosaic using Geospatial Data Abstraction Layer (GDAL) software (GDAL, Version 1.11.0, www.GDAL.org).

Mosaicked imagery was first processed by a human observer to obtain manual counts and locations of all avian species present. Identifying avian species from the collected imagery was rather straightforward due to the uniformity of the shape and color of aquaculture ponds as well as the lack of vegetation. However, in the event an individual bird was difficult to identify, a second observer would examine the image, and a decision was made by both observers on the identification. Two different automated pattern recognition algorithms, color segmentation and template matching (discussed below), were then applied to the mosaics to identify and count individual birds. All counts were summed on a per-pond basis, as that is the unit of interest with respect to potential impacts to production.

We evaluated the accuracy of each method at each height AGL and for each species using various metrics. These metrics were the mean observer count per pond compared to the mean algorithm count per pond, the mean percent of omission errors, and mean percent of commission errors. Observer count was divided by the algorithm count to acquire an overall accuracy metric of the algorithms. A value of 1 for this accuracy estimate indicates a perfect match between the observer count and algorithm count, while >1 indicates underestimation of the algorithm and <1 indicates overestimation. Omission percent is calculated by dividing the number of birds the algorithm failed to identify by the actual count and multiplying by 100. Commission percent is calculated by dividing the number falsely identified birds by the algorithm count and multiplying by 100 (Abd-Elrahman et al. 2005).

The sample size was not large enough to statistically determine both the influence of height AGL and species on the accuracy of the algorithms. We therefore combined all species and ran an ANOVA for each algorithm using height AGL as the independent factor and accuracy as the dependent variable. We also ran an ANOVA for each algorithm using species as the independent factor (height AGL lumped together) and accuracy as the dependent variable to determine potential differences in accuracy among species.

These models were run using type II sums of squares to cope with the unbalanced nature of

the data (Langsrud 2003). Model assumptions were checked visually using residual plots. Any significant results were then followed by a Tukey's post hoc test to determine significant difference among levels. These tests were done to determine general differences in overall accuracy between observer count and algorithm count without considering omissions or commissions. For each species, we combined heights AGL and ran a paired Mann-Whitney-Wilcoxon test to determine differences in percent omission and commission between methods for every pond. This nonparametric test was chosen due to the data violating the assumption of normality (Fay and Proschan 2010). All statistical analysis was conducted in Program R, version 3.5.1 (R Core Team 2018), and statistical significance was assessed using an alpha of 0.05.

Color segmentation algorithm

The Delta-E (ΔE) color segmentation algorithm (Chen et al. 2004, Baldevbhai and Anand 2012) was used to extract the silhouettes of birds from the UAS-collected image mosaics. Greek letter delta (Δ) is commonly used to represent the difference, and E stands for *Empfindung* in German, meaning "sensation." Therefore, ΔE means "a difference in sensation." This algorithm seeks to find the difference between pixels in the training set and pixels in the test imagery. With the UAS image mosaic being the test image, a ΔE value of <1.0 represents the case where the training and test pixels are nearly indistinguishable. The higher the value of ΔE, the larger the color difference between training and test samples. In our case, the UAS-collected visible imagery has red (R), green (G), and blue (B) wavelength bands. However, ΔE is developed to work best in the "Lab" color space, where the color coordinate "L" stands for lightness and "a" and "b" represent color-opponent dimensions based on nonlinearly compressed coordinates. Lab color space is known to approximate human vision as the L component is developed to be similar to human perception of lightness. The RGB wavelength bands work better to model color on physical devices such as computer or television displays rather than human perception.

The value ΔE is defined by International Commission on Illumination (CIE 1976)

and was used to compute the segmentation thresholds. The visible image with R, G, and B bands are first converted to CIELAB color space using the formulas defined in Baldevbhai and Anand (2012). A color image pixel in CIELAB is represented as 3 components: L for the lightness, and color components a for green-red and b for blue-yellow. Chroma (Cab) and Hue (Hab) were derived from L a b by using equations (1) and (2).

$$C_{ab} = \sqrt{a^2 + b^2} \quad (1)$$

$$H_{ab} = \tan^{-1}\left(\frac{b}{a}\right) \quad (2)$$

For a set of training (L_{tr}, a_{tr}, b_{tr}) and test ($L_{tst}, a_{tst}, b_{tst}$) pixels, ΔE can be computed by using equation (3):

$$\Delta E = \sqrt{\left(\frac{(L_{tr} - L_{tst})}{K_L}\right)^2 + \left(\frac{(C_{tr} - C_{tst})}{1 + K_1 C_1}\right)^2 + \left(\frac{(\Delta H_{ab})}{1 + K_2 C_2}\right)^2} \quad (3)$$

where,

$$\Delta H_{ab} = \sqrt{(a_{tr} - a_{tst})^2 + (b_{tr} - b_{tst})^2 - \Delta C_{ab}^2}$$

$$C_1 = \sqrt{a_{tr}^2 + b_{tr}^2} \text{ and } C_2 = \sqrt{a_{tst}^2 + b_{tst}^2}$$

K_L, K_1 and K_2 are weighting factors that are set to 1.5, 0.045, and 0.015, respectively.

After the conversion into the Lab color space, ΔE is calculated for each pixel in the mosaic. The computation of ΔE is then followed by histogram computation of this color difference to find a threshold. The algorithm requires manual selection of the color of the target object that needs to be segmented in the first step (training data; Kumar et al. 2016). A connected component object counting algorithm is then used to accurately count the segmented objects, resulting in the estimation of number of birds in the imagery.

Template matching algorithm

Template Matching is a computer vision method that allows the identification of objects in an image that matches a verified image pattern (Sahani et al. 2011). It is especially useful for finding regions of an image that match (are similar) to a template (training or example) image. The algorithm requires a

template image and a test image in which we seek to find a match to the template image. The template image contains the object or bird that we are interested in identifying within the test image. The goal is to find the best-matched regions with the highest value of the underlying matching metric. Several metrics are used in the literature; the popular ones are (1) sum of squared differences, or SSD; (2) normalized sum of squared differences, or NSSD; (3) cross-correlation, or CC; or (4) normalized cross-correlation, or NCC. In our implementation, NCC is used as an underlying metric to estimate the similarity of an image region to the template.

We refer the search image and test image as S and T, respectively. Let the size of S be NxN and the size of T be MxM, where N>M. The template matching process starts with registering T at the top left corner of S at the pixel location of ($x = 1$, $y = 1$) and continues shifting the T a pixel at a time in a push-broom scanning fashion. The NCC function between T and the corresponding pixels in S at a point (u,v) is given by equation (4):

$$NCC(u,v) = \frac{\sum_{x=1}^{M}\sum_{y=1}^{M}[S(u+x,v+y)T(x,y) - M^2 S(u,v)\bar{T}]}{\sqrt{[\sum_{x=1}^{M}\sum_{y=1}^{M} S^2(u+x,v+y) - M^2\bar{S}^2(u,v)][\sum_{x=1}^{M}\sum_{y=1}^{M} T^2(x,y) - M^2\bar{T}^2]}} \quad (4)$$

where $\bar{S}$ and $\bar{T}$ are the mean of S and T images respectively and are given by

$$\bar{S}(u,v) = \frac{1}{M^2}\sum_{x=1}^{M}\sum_{y=1}^{M} S(u+x, v+y)$$

$$\bar{T}(u,v) = \frac{1}{M^2}\sum_{x=1}^{M}\sum_{y=1}^{M} T(x,y)$$

The NCC is computed by using equation (4) bounded to (-1,+1), with +1 indicating 100% match, 0 indicating no match, and -1 indicating 100% inverse match (matching with the negative of the template). To achieve both rotation and scale invariance, the template image is further scaled and rotated to compute NCC to identify fish-eating birds from the mosaicked imagery. This allowed finding the template occurrences in the source image regardless of its orientation, scale, or size. This method uses a pyramid search that was adapted to allow multi-angle and multi-scale matching that can find the rotated and scaled instances of the template. Pyramid search identifies template position and orientation and estimates the matching metric.

Results

Among the 52 ponds flown during the 4 separate surveys, 26 ponds contained our target species and were used for automated image analysis. Overall mean (+SD) correct classification (observer count divided by algorithm count) with species and heights AGL combined were 0.80 (0.58) for template matching and 0.67 (0.67) for color segmentation. Accuracy varied considerably among species but was best overall for egrets (Tables 1 and 2). Egrets were also the most observed species in this study and were therefore more influential on our overall correct classification rate reported compared to either herons or cormorants.

There was no significant difference in accuracy among heights AGL when all species were lumped together for either template matching ($F_{2, 53} = 0.02$, $P = 0.98$) or color segmentation ($F_{2, 53} = 0.82$, $P = 0.45$). Mean template matching accuracy was 0.79 (0.41) at 61 m AGL, 0.81 (0.59) at 122 m, and 0.78 (0.73) at 183 m. Mean color segmentation accuracy was 0.48 (0.52) at 61 m AGL, 0.76 (0.71) at 122 m, and 0.71 (0.73) at 183 m. There was a significant difference in accuracy among species when all heights AGL were combined for template matching ($F_{2, 53} = 10.30$, $P = 0.0001$). The Tukey's test revealed mean accuracy to differ between egrets and cormorants ($P = 0.01$), egrets and herons ($P = 0.04$), and cormorants and herons ($P = 0.0002$). Mean accuracy for template matching was 0.44 (0.36) for cormorants, 0.88 (0.49) for egrets, and 1.37 (0.80) for herons. There was also a significant result for color segmentation among species ($F_{2, 53} = 8.59$, $P = 0.0005$), with Tukey's test results revealing egret accuracy to be different than cormorants ($P = 0.04$) and herons ($P = 0.0007$). Color segmentation overestimated herons and cormorants compared to egrets with a mean accuracy of 0.02 (0.04) for herons, 0.95 (0.35) for egrets, and 0.52 (0.92) for cormorants.

Egrets were the most frequently observed species, being found on 6 ponds at 61 m AGL, 17 ponds at 122 m, and 6 ponds at 183 m (Tables 1 and 2). Color segmentation had significantly lower average omission ($P = 0.003$) and commission ($P = 0.0001$) percentages than template matching. Median omission and commission percent was 0.30 and 0.43 for template matching, and 0.12 and 0.15 for color segmentation, respectively. Actual counts versus algorithm counts were

Table 1. Results from a template matching algorithm used to identify 3 fish-eating bird species, double-crested cormorants (*Phalacrocorax auritus*), great blue herons (*Ardea herodias*), and great egrets (*A. alba*) at 3 different heights above ground level (AGL) on catfish (*Ictalurus* spp.) aquaculture ponds in Mississippi, USA. This algorithm was applied to mosaicked imagery constructed from individual overlapped images captured by an unmanned aerial system. Numbers presented are *n* = number of ponds, mean, and standard deviation in parentheses.

Species	*n*	AGL (m)	Observer count	Algorithm count	Accuracy[a]	Percent omission[b]	Percent commission[c]
	6	61	32.7 (25.8)	37.7 (38.5)	0.99 (0.24)	21.2 (14.6)	22.7 (17.7)
Egret	17	122	16.2 (17.1)	19.8 (15.6)	0.87 (0.59)	50.8 (29.7)	56.2 (33.7)
	6	183	19.0 (25.9)	21.3 (24.2)	0.76 (0.34)	14.6 (14.2)	38.5 (20.6)
	4	61	4.5 (5.7)	8.5 (14.3)	0.98 (0.44)	10.3 (15.8)	15 (30)
Heron	3	122	2.3 (1.5)	1.7 (0.6)	1.33 (0.58)	12.6 (28.9)	0 (0)
	1	183	3 (na)	1 (na)	3 (na)	66.7 (na)	0 (na)
	5	61	17.8 (6.6)	72.4 (60.0)	0.38 (0.26)	21.5 (15.0)	69.4 (22.5)
Cormorant	6	122	18.8 (14.8)	57.0 (26.8)	0.39 (0.33)	28.9 (19.2)	73.5 (17.6)
	8	183	16.0 (16.8)	39.9 (28.9)	0.51 (0.45)	31.1 (21.5)	70.1 (20.4)

[a] Accuracy is calculated by dividing observer counts by algorithm counts.
[b] Percent omission is calculated by dividing the number of birds the algorithm failed to identify by the actual count and multiplying by 100.
[c] Percent commission is calculated by dividing the number of falsely identified birds by the algorithm count and multiplying by 100.

Table 2. Results from a color segmentation algorithm used to identify 3 fish-eating bird species, double-crested cormorants (*Phalacrocorax auritus*), great blue herons (*Ardea herodias*), and great egrets (*A. alba*) at 3 different heights above ground level (AGL) on catfish (*Ictalurus* spp.) aquaculture ponds in Mississippi, USA. This algorithm was applied to mosaicked imagery constructed from individual overlapped images captured by an unmanned aerial system. Numbers presented are *n* = number of ponds, mean, and standard deviation in parentheses.

Species	*n*	AGL (m)	Observer count	Algorithm count	Accuracy[a]	Percent omission[b]	Percent commission[c]
	6	61	32.7 (25.8)	30.8 (25)	1.04 (0.15)	19.8 (15.2)	17.6 (11)
Egret	17	122	16.2 (17.1)	20.3 (18.4)	0.86 (0.34)	12.3 (13.3)	25.4 (30)
	6	183	19 (25.9)	15 (16.6)	1.10 (0.47)	17.6 (18.5)	15.4 (28)
	4	61	4.5 (5.7)	1491.8 (1340.6)	0.03 (0.05)	1.9 (3.8)	97.0 (5.4)
Heron	3	122	2.3 (1.5)	514 (419)	0.01 (0.01)	0 (0)	99.2 (1)
	1	183	3 (na)	110 (na)	0.03 (na)	0 (na)	97.3 (na)
	5	61	17.8 (6.6)	1865.6 (2261.1)	0.17 (0.34)	22.3 (27.6)	85.2 (30.6)
Cormorant	6	122	18.8 (14.8)	232.0 (251.8)	0.83 (1.35)	24.0 (32.8)	68.7 (32.5)
	8	183	16.0 (16.8)	111.5 (149.3)	0.50 (0.80)	29.8 (34.0)	83.0 (13.3)

[a] Accuracy is calculated by dividing observer counts by algorithm counts.
[b] Percent omission is calculated by dividing the number of birds the algorithm failed to identify by the actual count and multiplying by 100.
[c] Percent commission is calculated by dividing the number of falsely identified birds by the algorithm count and multiplying by 100.

comparable; however, this is due to omissions and commissions being similar (Table 1 and 2). Essentially, each algorithm misidentified egrets close to the same rate as it failed to identify egrets. Figure 1A shows an example of visual spectrum imagery of egrets used for performing color segmentation, and Figure 1B is the resulting output.

Herons were digitally captured on imagery on 4 ponds at 61 m AGL, 3 ponds at 122 m, and only 1 pond at 183 m. Average omission percentage of template matching was not significantly different from color segmentation (P = 0.18), but commission percentages were significantly less than color segmentation (P = 0.008). Median omission and commission percent was 0.04 and 0.0 for template matching, and 0.0 and 0.99 for color segmentation, respectively. Although the omissions were approximately zero for color segmentation, commission percent was nearly 100% (Tables 1 and 2). In effect, color segmentation could not accurately differentiate between the color of cryptic herons and the background, leading the algorithm to classify almost everything in the image as a heron. Figure 2A shows visual spectrum imagery of egrets and herons, which was used for performing template pattern matching. Figures 2B shows an example of the results of template matching of herons from the selected imagery.

Cormorants were observed on 5 ponds at 61 m AGL, 6 ponds at 122 m, and 8 ponds at 183 m. We unfortunately experienced issues with mosaic artifacts due to the larger pond sizes found at study areas 2 and 3 relative to study area 1. The lack of features to align imagery for mosaicking resulted in issues with image overlap and distortion during the stitching process. We therefore subset some images to smaller areas within ponds that contained cormorants and for which image quality issues associated with mosaicking were largely removed. Despite the sub-setting, neither algorithm performed well for this species, each having both elevated omission and commission percentages. No significant difference was detected between methods for either omission percentage (P = 0.89), or commission percentage (P = 0.10). Median omission and commission percent was 0.20 and 0.77 for template matching, and 0.11 and 0.91 for color segmentation, respectively.

Mean algorithm count was greatly elevated compared to actual count (Tables 1 and 2). Figure 3A shows an example of visual spectrum imagery containing cormorants used in color segmentation that performed well, and Figure 3B is the resulting output.

Discussion

Using UAS, we were able to successfully collect imagery of fish-eating birds on catfish aquaculture ponds and estimate abundances using manual counting. When applying computer-automated algorithms to this imagery, we observed varying levels of accuracies, which were dependent on the species observed, the algorithm used, and ambient conditions. Overall, the algorithms were able to correctly distinguish fish-eating bird species that were distinctly different in terms of color and morphology. Our sample size for each species at each height AGL was low, and we therefore cannot establish any real difference in algorithm
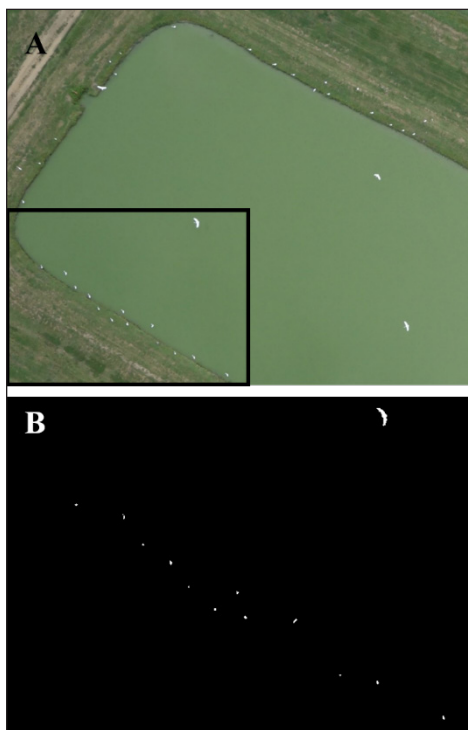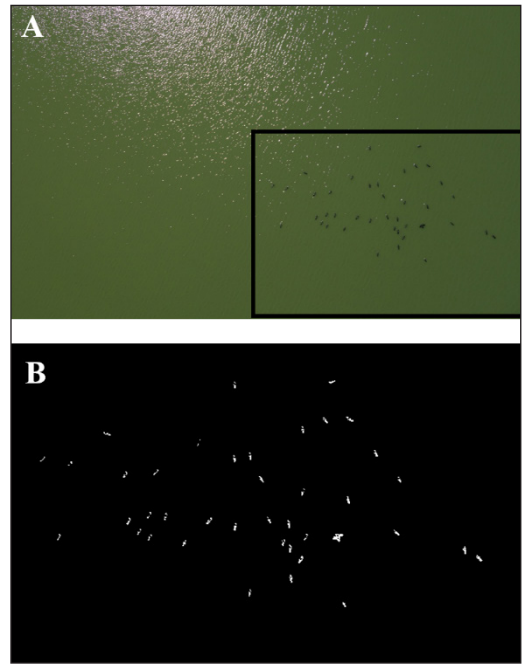

Figure 1. (A) Visual spectrum imagery of great egrets (*Ardea alba*) on a catfish (*Ictalurus* spp.) aquaculture pond in Mississippi, USA, taken on August 9, 2017. This imagery was taken using a Sony RX100 camera attached to a Triton unmanned aerial system at 61 m above ground level. (B) Results of a color segmentation algorithm specific to great egrets for the area outlined in (A).
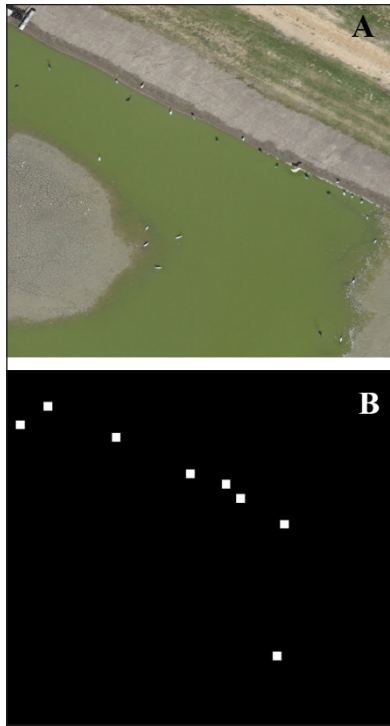
Figure 2. (A) Visual spectrum imagery of great egrets (*Ardea alba*) and great blue herons (*A. herodias*) on a catfish (*Ictalurus* spp.) aquaculture pond in Mississippi, USA, taken on October 18, 2014. This imagery was taken using a Sony RX100 camera attached to a Triton unmanned aerial system at 61 m above ground level. (B) Results of the template matching algorithm specific to great blue herons for the area in (A).

Figure 3. (A) Visual spectrum imagery of double-crested cormorants (*Phalacrocorax auritus*) on a catfish (*Ictalurus* spp.) aquaculture pond in Mississippi taken on August 8, 2014. This imagery was taken using a Sony RX100 camera attached to a Triton unmanned aerial system at 122 m above ground level. (B) Results of the Delta-E color segmentation algorithm specific to double-crested cormorants for the area outlined in (A).

performance based on height AGL or resolution for each species.

We found no difference in accuracy among heights AGL when lumping species together for either algorithm; however, differences among species at differing heights are probable given their differences in morphology. Manual counting of mosaics was possible for each height AGL. However, mosaics at 183 m were quite pixelated, making identification more time consuming and complicated compared to the other heights AGL. Imagery collected at 61 m AGL produced the highest resolution; however, these flights also took the longest time to complete, required the greatest amount of memory to store imagery, and had more mosaicking issues than other heights AGL. Because of these reasons, we recommend using a height AGL that produces image quality high

enough for easy manual counting but does not require long flight times or large amounts of memory. In this study with our UAS setup, the 122 m AGL best met these goals.

We found both color segmentation and template matching to perform well on egrets, template matching performed better than color segmentation for herons, and both algorithms performed poorly for cormorants. Overall accuracy was measured by dividing actual counts by algorithm counts, resulting in a metric that is ideally close to 1. However, it is important to note differences in both omissions and commissions, as these relate directly to the ability of the algorithms to successfully detect target species as well as its ability to avoid false detections. We found similar rates of omissions and commissions on a number of ponds for different species that can, in a sense, average

out and thus produce estimates that are close to actual counts in some instances.

With our algorithms and fieldwork, we identified 4 major factors that can influence results: (1) morphological and behavioral characteristics of the birds themselves, (2) sun reflections on the waterbody, (3) bird shadows, and (4) mosaicking artifacts. Morphological characteristics such as size, shape, and color of the target species can influence the performance of automated algorithms (Chabot and Francis 2016, Rush et al. 2018). This was evident in the case of color with egrets, which stood out starkly in the imagery, increasing accuracy of the color segmentation algorithm. Behavioral characteristics, such as foraging behavior, will affect where the target species is located in the environment. In our case, herons and egrets both forage along shorelines, while cormorants forage in open water. This results in differing backgrounds in which the algorithm needs to identify specific target species. Additionally, specific habitat will also add complexity to identifying birds. For example, identifying herons on aquaculture is likely easier compared to a more diverse and complex tidal marsh.

Reflections caused by sun on the waterbody can be a major issue, as the imagery gets saturated and the algorithms are not sensitive enough to identify the birds accurately. This can be seen where the reflection from the sun has caused noise in the imagery (Figure 3). Any white bird within that region may go unidentified, or conversely, white reflections can be misclassified as a bird, resulting in a high omission rate. This issue did occur in our work when identifying egrets while there was bright sun reflectance off of pond water, which was a similar white color to the birds. Shadows cast by birds are not a major problem with color segmentation algorithm, as it relies on the red, green, and blue combination of pixels rather than shape. With the template matching algorithm, shadows can sometimes (based on its similarity to the bird) be misclassified as a bird. Finally, the image mosaics were created by stitching overlapping image snapshots captured from the UAS. These individual snapshots need to have object features or tie points that can be used for stitching as features. This was a problem for cormorants at study area 2 and 3. Specifically, ponds were so

large that mosaicking was difficult due to the absence of common points among individual images. Additionally, with waterbody being monotonous, there can be some artifacts in the mosaics along the stitching line that can influence the algorithm classification.

Color segmentation is a fast and not computationally intensive method for identifying wildlife that tend to be monotypic in color and that have strong contrasts against the image background. Color segmentation is particularly suitable for surveys taking place at catfish aquaculture facilities, as background colors are particularly uniform and contrast nicely against the white color of egrets and sometimes the black color of cormorants. However, in situations where the background contains colors similar to that of the target species, color segmentation may produce false identification.

Herons were especially difficult for this problem, with the color segmentation results showing nearly 100% commission. Herons appear light grey in color on the imagery, and the algorithm was not sensitive enough to differentiate them from the shoreline background effectively. Similarly, the cormorants we captured on imagery tended to be on ponds with darker, murkier water, reducing identification accuracy. In contrast, template matching algorithms can be employed to identify birds based on shape, and thus may perform better with more cryptic wildlife such as the case with herons in our study. Although template matching accuracy was better for herons compared to color segmentation, we observed a very limited number of herons throughout this study. Therefore, general claims about template matching performance on herons is difficult, especially in cases where heron abundance is greater. Template matching performed similarly to color segmentation for cormorants. When cormorants sit on open water, they are oval in shape, and mosaic artifacts and wave ripples seemed to match the shape, causing commissions. Nonetheless, template matching is much more computationally intensive in comparison to color segmentation, creating a tradeoff between computer processing time and potential accuracy, especially on larger images.

The use of UAS in ecological work continues

to grow as the technology advances, their user-friendliness increases, and their costs decline (Anderson and Gaston 2013, Christie et al. 2016, Gonzalez et al. 2016). With UAS ability to take high-resolution imagery, the development of automated pattern recognition has unsurprisingly also become a popular tool to identify wildlife (Chabot and Francis 2016). Whereas larger mammalian studies have traditionally used this technology more in the past due to the larger size of target species, monitoring smaller species, such as birds, is now possible (Linchant et al. 2015, Chabot and Francis 2016). A similar but more sophisticated method than what is presented here is object-based image analysis (OBIA; Blaschke 2010). Commercial products of OBIA software are becoming more readily available and user-friendly for the use of identifying features of interest in aerial imagery based on spatial, spectral, and texture attribute (Chabot et al. 2018). Chabot et al. (2018) used off-the-shelf OBIA software to develop a repeatable method using OBIA on aerial imagery and tested it on lesser snow geese (*Chen caerulescens*) imagery taken across the Canadian Arctic with impressive accuracy.

As technological advances continue to be made, UAS platforms and computer-based algorithms will have countless more applications in wildlife ecology. The UAS are already being used in a variety of creative ways in the field. Wilson et al. (2017) attached a recording device to a rotary UAS as a means of recording songs birds in replacement of traditional point count methods. The UAS are also showing promise as bird harassment tools to reduce agriculture damage (Bhusal et al. 2018, Wandrie et al. 2019) and to actively herd birds away from certain areas (Paranjape et al. 2018). Interestingly, there is a fine line between using UAS to harass purposely, or to discreetly monitor avian species.

Numerous studies have explicitly tested or at least reported on bird responses to UAS, all which show varying degrees of responses, ranging from no response at all to complete flushing of the bird. However, these responses are very specific to certain factors, such as specific species, time of day, reproductive status, and height flown above the animal (Brisson-curadeau et al. 2017, Sardà-palomera

et al. 2017, Weimerskirch et al. 2017). Some of the current restrictions of UAS use in this field include limited coverage area due to battery constraints and restricted legislation (Linchant et al. 2015). As strides are made to address these challenges, it is clear that UAS will revolutionize data collection in many aspects of ecological research and management.

Management implications

Here we were able to apply UAS and automated counting algorithm technologies to estimate the number of fish-eating birds on aquaculture facilities. Although our results varied in accuracy depending on the species and algorithm, this application to identify birds on catfish ponds has the potential applications to monitor human–wildlife conflict between fish-eating birds and catfish producers. These methods can rapidly count and identify specific target species with minimal disturbance to the wildlife over relatively large areas and provide near real-time data on both bird locations and total abundance. Such information can be applied to management efforts to reduce depredation, provide estimates to be used in damage estimates and crop insurance claims, and acquire data on bird foraging ecology.

Acknowledgments

Literature cited

Abd-Elrahman, A., L. Pearlstine, and F. Percival. 2005. Development of pattern recognition algorithm for automatic bird detection from unmanned aerial vehicle imagery. Surveying and

Land Information Science 65:37–45.

Anderson, K., and K. J. Gaston. 2013. Lightweight unmanned serial vehicles will revolutionize spatial ecology. Frontiers in Ecology and the Environment 11:138–146.

Bakó, G., M. Tolnai, and Á. Takács. 2014. Introduction and testing of a monitoring and colony-mapping method for waterbird populations that uses high-speed and ultra-detailed aerial remote sensing. Sensors 14:12828–12846.

Baldevbhai, P. J., and R. S. Anand. 2012. Color image segmentation for medical images using L*a*b* color space. Journal of Electronics and Communication Engineering 1:24–45.

Bhusal, S., K. Khanal, M. Karkee, K. Steensma, and M. E. Taylor. 2018. Unmanned aerial systems (UAS) for mitigating bird damage in wine grapes. Proceedings of the 14th International Conference on Precision Agriculture, Montreal, Quebec, Canada.

Blaschke, T. 2010. Object based image analysis for remote sensing. ISPRS Journal of Photogrammetry and Remote Sensing 65:2–16.

Brisson-curadeau, É., D. Bird, C. Burke, D. A. Fifield, P. Pace, R. B. Sherley, and K. H. Elliott. 2017. Seabird species vary in behavioural response to drone census. Scientific Reports 7:1–9.

Chabot, D., C. Dillon, and C. M. Francis. 2018. An approach for using off-the-shelf object-based image analysis software to detect and count birds in large volumes of aerial imagery. Avian Conservation and Ecology 13:15.

Chabot, D., and C. M. Francis. 2016. Computer-automated bird detection and counts in high-resolution aerial images: a review. Journal of Field Ornithology 87:343–359.

Chen, H., W. Chien, and S. Wang. 2004. Contrast-based color image segmentation. IEEE Signal Processing Letters 11:641–644.

Christie, K. S., S. L. Gilbert, C. L. Brown, M. Hatfield, and L. Hanson. 2016. Unmanned aircraft systems in wildlife research: current and future applications of a transformative technology. Frontiers in Ecology and the Environment 14:241–251.

Dorr, B. S., L. W. Burger, and S. C. Barras. 2008. Evaluation of aerial cluster sampling of double-crested cormorants on aquaculture ponds in Mississippi. Journal of Wildlife Management 72:1634–1640.

Dorr, B. S., L. W. Burger, S. C. Barras, and K. C. Godwin. 2012. Economic impact of double-crested cormorant, *Phalacrocorax auritus*, depredation on channel catfish, *Ictalurus punctatus*, aquaculture in Mississippi, USA. Journal of the World Aquaculture Society 43:502–513.

Fay, M. P., and M. A. Proschan. 2010. Wilcoxon-Mann-Whitney or t-test? On assumptions for hypothesis tests and multiple interpretations of decision rules. Statistics Surveys 4:1–39.

Frederick, P. C., T. Towles, R. J. Sawicki, and G. T. Bancroft. 1996. Comparison of aerial and ground techniques for discovery and census of wading bird nest colonies. Condor 98:837–841.

Glahn, J. F., and K. E. Brugger. 1995. The impact of double-crested cormorant on the Mississippi Delta catfish industry: a bioenergetics model. Colonial Waterbirds 18:168–175.

Glahn, J., and D. T. King. 2004. Bird Depredation. Pages 634–657 *in* C. S. Tucker and J. Hargreaves, editors. Biology and culture of channel catfish. Volume 34. Elsevier B.V., Amsterdam, Netherlands.

Glahn, J., M. E. Tobin, and B. F. Blackwell. 2000. A science-based initiative to manage double-crested cormorant damage to southern aquaculture. APHIS 11-55-010, U.S. Department of Agriculture, Animal and Plant Health Inspection Service, Wildlife Services' National Wildlife Research Center, Fort Collins, Colorado, USA.

Gonzalez, L. F., G. A. Montes, E. Puig, S. Johnson, K. Mengersen, and K. J. Gaston. 2016. Unmanned aerial vehicles (UAVs) and artificial intelligence revolutionizing wildlife monitoring and conservation. Sensors 16:1–18.

Green, M. C., M. C. Luent, T. C. Michot, C. W. Jeske, and P. L. Leberg. 2008. Comparison and assessment of aerial and ground estimates of waterbird colonies. Journal of Wildlife Management 72:697–706.

Han, Y., S. H. Yoo, and O. Kwon. 2017. Possibility of applying unmanned aerial vehicle (UAV) and mapping software for the monitoring of waterbirds and their habitats. Journal of Ecology and Environment 41:1–7.

Hodgson, J. C., S. M. Baylis, R. Mott, A. Herrod, and R. H. Clarke. 2016. Precision wildlife monitoring using unmanned aerial vehicles. Scientific Reports 6:1–7.

Hodgson, J. C., R. Mott, S. M. Baylis, T. T. Pham, S. Wotherspoon, A. D. Kilpatrick, R. R. Segaran, I. Reid, A. Terauds, and L. P. Koh. 2018. Drones count wildlife more accurately and pre-

cisely than humans. Methods in Ecology and Evolution 1160–1167.

Kumar, V., T. Lal, P. Dhuliya, and D. Pant. 2016. A study and comparison of different image segmentation algorithms. Proceedings of the 2016 2nd International Conference on Advances in Computing, Communications, & Automation (ICACCA, Fall). Bareilly, Uttar Pradesh, India.

Langsrud, O. 2003. ANOVA for unbalanced data: use type II instead of type III sums of squares. Statistics and Computing 13:163–167.

Linchant, J., J. Lisein, J. Semeki, P. Lejeune, and C. Vermeulen. 2015. Are unmanned aircraft systems (UASs) the future of wildlife monitoring? A review of accomplishments and challenges. Mammal Review 45:239–252.

Mott, D., and M. Brunson. 1995. A historical perspective of catfish production in the southeast in relation to avian predation. Paper 24, Proceedings of the 7th Eastern Wildlife Damage Management Conference, Jackson, Mississippi, USA.

National Agricultural Statistics Service (NASS). 2015. Catfish production. United States Department of Agriculture, National Agriculture Statistics Service 1–10.

Paranjape, A. A., S. Chung, K. Kim, and D. H. Shim. 2018. Robotic herding of a flock of birds using an unmanned aerial vehicle. IEEE Transactions on Robotics 1–15.

R Core Team. 2018. R: a language and environment for statistical computing. R Foundation for Statistical Computing, Vienna, Austria.

Rush, G. P., L. E. Clarke, M. Stone, and M. J. Wood. 2018. Can drones count gulls? Minimal disturbance and semiautomated image processing with an unmanned aerial vehicle for colony-nesting seabirds. Ecology and Evolution 1–13.

Sahani, S. K., G. Adhikari, and B. Das. 2011. A fast template matching algorithm for aerial object tracking. Proceedings of the 2011 International Conference on Image Information Processing, Waknaghat, Shimla, India.

Samiappan, S., G. Turnage, L. Casagrande, P. Stinson, and R. Moorhead. 2017. Using unmanned aerial vehicles for high-resolution remote sensing to map invasive *Phragmites australis* in coastal wetlands. International Journal of Remote Sensing 38:2199–2217.

Sardà-palomera, F., G. Bota, N. Padilla, L. Brotons, and F. Sardà. 2017. Unmanned aircraft systems to unravel spatial and temporal factors affecting dynamics of colony formation and nesting success in birds. Journal of Avian Biology 48:1273–1280.

Sasse, D. 2003. Job-related mortality of wildlife workers in the United States, 1937–2000. Wildlife Society Bulletin 31:1015–1020.

Tucker, C., and J. Hargreaves. 2004. Biology and culture of channel catfish. Elsevier B.V., Amsterdam, Netherlands.

U.S. Department of Agriculture. USDA. 2010. Catfish 2010 part III: changes in catfish health and production practices in the United States, 2002–09. Technical document #597.1212. U.S. Department of Agriculture, Animal Plant Health Inspection Service, Veterinary Services, Centers of Epidemiology and Animal Health, National Health Monitoring System, Fort Collins, Colorado, USA.

Vilsack, T., and J. T. Reilly. 2014. 2012 Census of aquaculture. Volume 3, Part 2, AC-12-SS-2. United States Department of Agriculture, National Agricultural Statistics Service, Washington, D.C., USA.

Wandrie, L. J., P. E. Klug, and M. E. Clark. 2019. Evaluation of two unmanned aircraft systems as tools for protecting crops from blackbird damage. Crop Protection 117:15–19.

Weimerskirch, H., A. Prudor, and Q. Schull. 2017. Flights of drones over sub-antarctic seabirds show species- and status-specific behavioural and physiological responses. Polar Biology 1–8.

Wilson, A. M., J. Barr, and M. Zagorski. 2017. The feasibility of counting songbirds using unmanned aerial vehicles. Auk 134:350–362.

Associate Editor: Larry Clark

Human–Wildlife Interactions 13(2)

PAUL C. BURR is a research assistant at Mississippi State University, Department of Wildlife Fisheries and Aquaculture. He received his B.S. and M.S. degrees from the University of North Dakota and will receive his Ph.D. degree from Mississippi State University in August 2019. His research has focused primarily on avian ecology and human–wildlife conflicts.

SATHISHKUMAR SAMIAPPAN (photo unavailable) is an assistant research professor at the Geosystems Research Institute at Mississippi State University. He received his B.Eng. degree from Bharathiar University, his M.Tech degree from Amrita University, and Ph.D. degree from Mississippi State University. His 10+ year career with Mississippi State University has focused on remote sensing, image analysis, machine learning, and recently on the use of unmanned aerial systems in remote sensing of the environment.

LEE A. HATHCOCK is a data acquisitions coordinator at the Geosystems Research Institute at Mississippi State University (MSU), where he received his B.S. and M.S. degrees. He has been with MSU for >10 years, primarily working on image processing and analysis, camera calibration, data management, and embedded systems. His current work focuses on image processing and data management with respect to remote sensing using unmanned aerial systems.

ROBERT J. MOORHEAD is the director of the Geosystems Research Institute and the Northern Gulf Institute as well as a distinguished professor at Mississippi State University (MSU). He received his B.S. degree from Geneva College and his M.S. and Ph.D. degrees from North Carolina State University. His 30+ year career with MSU has focused on image processing, visualization of modeled and measured phenomenon, and more recently on the use of unmanned aerial systems in remote sensing of the environment.

BRIAN S. DORR is a research wildlife biologist with the U.S. Department of Agriculture, Wildlife Services, National Wildlife Research Center (NWRC), Mississippi Field Station and is an adjunct associate professor with Mississippi State University, Department of Wildlife Fisheries and Aquaculture. He received his B.S. degree from the University of Arizona and his M.S. and Ph.D. degrees from Mississippi State University. His 20+ year career with NWRC has focused on the ecology of predatory birds, particularly as it relates to wildlife damage management including fish-eating bird impacts to aquaculture.